Journal of Hazardous Materials 162 (2009) 860–865

Contents lists available at ScienceDirect

Journal of Hazardous Materials

journal homepage: www.elsevier.com/locate/jhazmat

Heterogeneous photo-Fenton degradation of polyacrylamide in aqueous solution over Fe(III)–SiO_2 catalyst

Ting Liu, Hong You*, Qiwei Chen

Department of Environmental Science and Engineering, Harbin Institute of Technology, P.O. Box 2606, 202 Haihe Road, Harbin 150090, PR China

ARTICLE INFO

Article history:
Received 29 December 2007
Received in revised form 8 April 2008
Accepted 22 May 2008
Available online 28 May 2008

Keywords:
Photo-Fenton
Polyacrylamide
Fe(III)–SiO_2 catalyst
Heterogeneous catalysis

ABSTRACT

This article presents preparation, characterization and evaluation of heterogeneous Fe(III)–SiO_2 catalysts for the photo-Fenton degradation of polyacrylamide (PAM) in aqueous solution. Fe(III)–SiO_2 catalysts are prepared by impregnation method with two iron salts as precursors, namely $Fe(NO_3)_3$ and $FeSO_4$, and are characterized by Brunauer–Emmett–Teller (BET), X-ray diffraction (XRD) and X-ray photoelectron spectroscopy (XPS) methods. The irradiated Fe(III)–SiO_2 is complexed with 1,10-phenanthroline, then is measured by UV–vis-diffuse reflectance spectroscopy (UV–vis-DRS) and XPS to confirm the oxidation state of Fe in solid state. By investigating the photo-Fenton degradation of PAM in aqueous solution, the results indicate that Fe(III)–SiO_2 catalysts exhibit an excellent photocatalytic activity in the degradation of PAM. Moreover, the precursor species and the OH^-/Fe mole ratio affect the photocatalytic activity of Fe(III)–SiO_2 catalysts to a certain extent. Finally, the amount of Fe ions leaching from the Fe(III)–SiO_2 catalysts is much low.

1. Introduction

"Produced water" is the largest volume of waste generated by the oil industry. In particular, with the application of polymer flooding technology in tertiary oil recovery processes in China, a kind of new produced water containing polyacrylamide (PAM), a high molecular weight polymer, have been produced. The conventional method to dispose of such produced water is either re-injected into the subsurface for permanent disposal or discharged directly to the marine environment. However, both methods have caused serious contamination to the ground water and surface water. On the other hand, the current physical treatment processes (settling separation and filtration) can not satisfy the treatment requirement. Hence, the treatment technologies of produced water containing PAM have become a key problem in oil industry in China.

Physical [1,2], biological [3,4] and chemical methods [5] are presently used for treatment of PAM. It was found that the degradation ratio of PAM in aqueous solution was slow by using biological methods. Recently, some investigators have reported the successful application of advanced oxidation processes for PAM degradation [6,7]. One of advanced oxidation processes, Fenton (a powerful source of oxidative $HO^{\bullet}$ generated from H_2O_2 in the presence of Fe^{2+} ions) or photo-Fenton reaction has been used in the degradation of many organic compounds [8,9]. Even though these systems are considered as a very effective approach to remove organic compounds, it should be pointed out that there is a major drawback because the post-treatment of Fe sludge is an expensive process. This shortcoming can be overcome by using heterogeneous photo-Fenton reaction. Therefore, a lot of effort has been made in developing heterogeneous photo-Fenton catalysts. For example, Parra et al. prepared Nafion/Fe structured membrane catalyst and used it in the photo-assisted immobilized Fenton degradation of 4-chorophenol [10]. However, Nafion/Fe structured membrane catalyst is much expensive for practical use. Thus, the low cost supports such as the C structured fabric [11,12], activated carbon [13], mesoporous silica SBA-15 [14–16], zeolite [17,18] and clay [19–21], have been used for the immobilization of active iron species. Remirez et al. prepared the catalysts using four iron salts as precursors for the heterogeneous Fenton-like oxidation of Orange II solutions [22]. The results showed that the nature of the iron salt had a significant effect on the process performance. So, it is necessary to discuss the photocatalytic activities of the catalysts by using different iron salts as precursors.

In this paper, a series of Fe(III)–SiO_2 catalysts were prepared at different OH^-/Fe mole ratio and by using two iron salts as precursors, namely $Fe(NO_3)_3$ and $FeSO_4$. All catalysts were characterized by BET, XRD and XPS. The oxidation state of Fe in the solid state was detected by the UV–vis-DRS and XPS measurement. The photocatalytic activity of Fe(III)–SiO_2 catalyst was evaluated in the photo-assisted Fenton degradation of PAM in aqueous solution in

* Corresponding author. Tel.: +86 451 86283118; fax: +86 451 86283118.
E-mail address: youhong@hit.edu.cn (H. You).

0304-3894/$ – see front matter © 2008 Elsevier B.V. All rights reserved.
doi:10.1016/j.jhazmat.2008.05.110

the presence of H_2O_2 and UV light at an initial solution pH of 6.8. The effects of the precursor species and the OH^-/Fe mole ratio on the photocatalytic activities of Fe(III)–SiO_2 catalysts were also studied. In addition, the leaching behavior of Fe from the catalyst surface was discussed.

2. Experimental

2.1. Materials

The analytical grade PAM, H_2O_2 (30%, w/w), $Fe(NO_3)_3{\cdot}9H_2O$, $FeSO_4{\cdot}7H_2O$, NaOH and 1,10-phenanthroline were used for this experiment without further purification. The average molecular weight of PAM was 5 000 000 Da and degree of hydrolysis of PAM was about 30%. Silica gel (40–60 mesh) as a support was purchased from Qingdao Ocean Chemical Company, China. The aqueous solution of PAM was prepared by dissolving a weighed quantity of PAM in distilled water.

2.2. Preparation of the catalysts

A series of catalysts were prepared by two methods as follows:

(1) Two catalysts were prepared by impregnation of 20 g silica gel in aqueous solution containing 0.05 mol/L $Fe(NO_3)_3$ and 0.05 mol/L $FeSO_4$, respectively and kept stirring for 6 h. After aging for 40 h at 105 °C, the samples were separated and washed several times with deionized water, then dried overnight at 80 °C. The dried samples were calcined at 500 °C for 5 h in an oven. Finally, two Fe(III)–SiO_2 catalysts were obtained, namely S-Fe^{3+} and S-Fe^{2+}.
(2) Twenty grams of silica gel carrier were first added into the aqueous solution containing 0.05 mol/L $Fe(NO_3)_3$ and 0.05 mol/L $FeSO_4$, respectively and kept under vigorous stirring for 2 h. Then, NaOH aqueous solution with different concentration was added drop by drop under stirring until the OH^-/Fe^{3+} or OH^-/Fe^{2+} mole ratio was equal to 1 and 2. After aging for 40 h at 105 °C, the solid product were separated and washed several times with deionized water and dried overnight at 80 °C. The dried samples were calcined at 500 °C for 5 h in an oven and the catalysts were named as S-Fe^{3+}/1, S-Fe^{3+}/2, S-Fe^{2+}/1 and S-Fe^{2+}/2, respectively.

2.3. Characterization of the catalysts

The iron content of Fe(III)–SiO_2 catalysts were verified by an inductively coupled plasma (ICP) (Model: Perkin-Elmer 5300 DV) after acidic digestion of the catalysts.

Brunauer–Emmett–Teller (BET) specific surface area, total pore volume and average pore size of synthesized Fe(III)–SiO_2 catalysts were measured by adsorption of nitrogen at 77 K, by using automated volumetric adsorption instrument (model Quantachrome Autosorb-1).

X-ray diffraction (XRD) measurement was employed using a Rigaku D/max-rB system with Cu Kα radiation operating at 45 kV and 40 mA. The 2θ ranged from 10 to 90°.

X-ray photo-electron spectroscopy (XPS) measurements were performed using a PHI 5700 spectrometer. The X-ray source was operated at 250 W and 12.5 kV and the C 1s signal was adjusted to 284.62 eV as the reference. The curve fitting was achieved by using a Physical Electronics PC-ACCESSESCA-V6.0E program with a Gaussian–Lorentzian sum function.

Finally, UV–vis-diffuse reflectance spectroscopy (UV–vis-DRS) measurements were recorded on TU1901 with a sphere reflectance accessory.

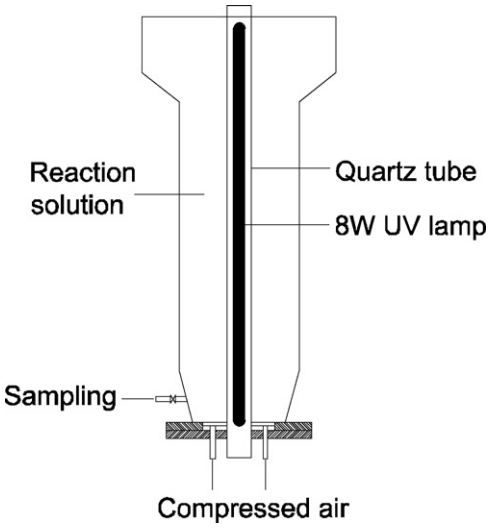

Fig. 1. Schematic diagram of three-phase fluidized bed photoreactor.

2.4. Catalytic activity

The photocatalytic activities of Fe(III)–SiO_2 catalysts were evaluated by degradation of PAM from aqueous solutions in a three-phase fluidized bed photoreactor (Fig. 1). The light source was UV lamp (Philips, 8 W, 254 nm) fixed inside of a cylindrical quartz tube. The total volume of PAM aqueous solution was 1500 mL. In order to ensure a good dispersion of Fe(III)–SiO_2 catalysts and good mixture in solution, compressed air was bubbled from the bottom at a flow rate of 3.3 L/min. For each experiment, the concentration of PAM and H_2O_2 were 100 and 200 mg/L, respectively. The catalyst loading was fixed at 1.0 g/L. The Fe(III)–SiO_2 catalyst and H_2O_2 were added into the photoreactor, at the same time, UV light was turned on and this was considered as the initial time for reaction. Then, samples were withdrawn at time intervals. The concentration of PAM in solution was measured by starch-CdI_2 spectrophotometry [23]. To determine mineralization of PAM solution, the total organic carbon (TOC) of the reaction solution was measured by a TOC-V_{CPN} Shimadzu TOC analyzer. In addition, the concentration of Fe in reaction solution was monitored by ICP.

2.5. Characterization of Fe(III)–SiO_2 after the reaction

In order to know the oxidation state of Fe on Fe(III)–SiO_2 catalyst surface under irradiation, the 1,10-phenanthroline was used which would be complexed with Fe(II)–SiO_2 in solid state [17]. 0.03% 1,10-phenanthroline and 0.6 mol/L acetate buffer (pH 8.60) was added into the photoreactor and the S-Fe^{2+}/1 catalyst was irradiated for 2 h. After reaction, the sample was filtered, washed several times and dried, then characterized by UV–vis-DRS and XPS measurement.

3. Results and discussion

3.1. Characterization of the catalysts before reaction

The content of Fe in Fe(III)–SiO_2 catalysts is shown in Table 1. It is observed that the Fe content in catalysts increases with the increase of OH^-/Fe mole ratio in both $Fe(NO_3)_3$ and $FeSO_4$ used as precursor. It should be mentioned that, with the increase of OH^-/Fe mole ratio, the structure of iron species in the solution develops from the low-molecular-weight species into high polymerization degree cationic polymer [24]. Therefore, with the increase of OH^-/Fe mole ratio,

Table 1
The content of Fe in catalysts and the results of BET tests

Samples	The content of Fe (wt.%)	BET surface area (m^2/g)	Total pore volume (cm^3/g)	Average pore width (Å)
SiO_2	0	419.0	0.93	88.9969
S-Fe^{3+}	0.404	446.0	0.99	88.7406
S-Fe^{3+}/1	0.496	462.0	1.02	88.4524
S-Fe^{3+}/2	0.684	470.0	1.04	88.2624
S-Fe^{2+}	0.184	442.6	0.98	88.6380
S-Fe^{2+}/1	0.534	411.8	0.99	96.5204
S-Fe^{2+}/2	0.976	314.9	1.07	135.8424

the polymerization degree of iron which was absorbed on SiO_2 carrier increased. It indicates that increasing OH^- concentration can improve the loading of Fe in Fe(III)–SiO_2 catalyst.

The BET surface area, total pore volume and average pore width of the investigated Fe(III)–SiO_2 catalysts are also listed in Table 1. The surface area of S-Fe^{3+} and S-Fe^{2+} catalysts were 446.0 and 442.6 m^2/g, respectively, higher than the SiO_2 carrier. When using $Fe(NO_3)_3$ as precursor, with the increase of OH^-/Fe mole ratio, the surface area and total pore volume of catalysts increased and the average pore width of catalysts changed a little. On the contrary, when using $FeSO_4$ as precursor, with the increase of OH^-/Fe mole ratio, the surface area of catalysts reduced, while the total pore volume of catalysts and the average pore width of catalysts increased. The results show that the pore structure of Fe(III)–SiO_2 catalysts prepared by the second method are affected remarkably by the precursor species and the OH^-/Fe mole ratio.

The XRD patterns of S-Fe^{3+}, S-Fe^{3+}/2, S-Fe^{2+} and S-Fe^{2+}/2 catalysts are illustrated in Fig. 2. The pattern showed a typical broad peak, which indicated that silica gel used as a support was a pure amorphous structure. On the other hand, the XRD patterns did not show iron oxides peaks, even for catalyst with 6.2 wt.% of iron (not shown in the figure). It may be proposed that the XRD techniques are not sensitive enough to detect little iron oxides because the higher background of XRD measurement caused by amorphous SiO_2.

The oxidation state of Fe on the surface of catalysts was characterized by XPS and the results are presented in Fig. 3. The binding energy of Fe $2p_{3/2}$ was determined to be 710.945 eV, 710.595 eV and 710.975 eV for S-Fe^{3+}, S-Fe^{3+}/1 and S-Fe^{3+}/2 catalyst, respectively, which was ascribable to Fe_2O_3 [25]. When $FeSO_4$ was used as the precursor, the Fe $2p_{3/2}$ peak was found at 711.195 eV, 711.345 eV and 711.850 eV for S-Fe^{2+}, S-Fe^{2+}/1 and S-Fe^{2+}/2 catalyst, respectively, strongly suggesting that the iron on the catalysts was Fe(III) [21]. When $FeSO_4$ was used as precursor, the binding energy of Fe $2p_{3/2}$ in catalysts were higher than that of catalysts prepared by $Fe(NO_3)_3$. It was difficult to give an adequate explanation of increasing in the binding energy of Fe $2p_{3/2}$ yet. O 1s survey scan further indicated the oxygen status on the catalyst surface. As shown in Fig. 4, the O 1s region can be fitted into four peaks, which are attributed to the chemisorbed oxygen, the lattice oxygen of SiO_2, the lattice oxygen of Fe_2O_3 and the chemically or physically adsorbed water. According to the reports [26,27], the chemisorbed oxygen can take an active part in the oxidation process and greatly improve the catalyst activity. It can be seen from Table 2 that the percentage of chemisorbed oxygen of catalyst was improved when $FeSO_4$ was used as precursor and the S-Fe^{2+}/1 catalyst had the highest percentage of chemisorbed oxygen.

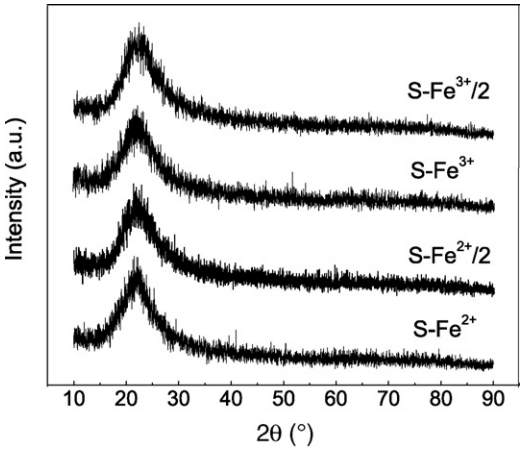

Fig. 2. XRD patterns of the Fe(III)–SiO_2 catalysts.

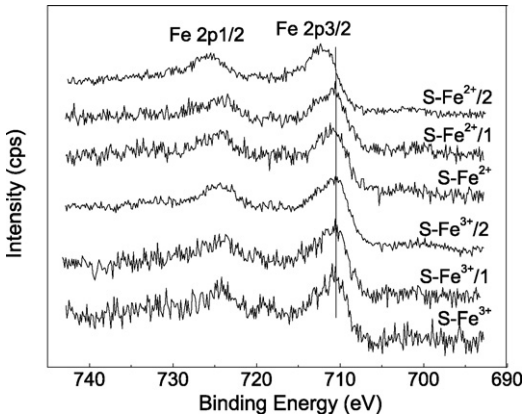

Fig. 3. XPS spectra of the Fe 2p region for the Fe(III)–SiO_2 catalysts.

3.2. Characterization of the catalysts after the reaction

The catalyst was characterized by UV–vis-DRS and XPS to confirm the formation of Fe(II)–SiO_2 when Fe(III)–SiO_2 was irradiated by photon. The UV–vis diffuse reflectance absorption spectra of Fe(III)–SiO_2 catalyst before and after reaction are shown in Fig. 5. The results clearly shows a new broad absorption band at 505–525 nm after irradiation which is characteristic band of $[Fe(1,10\text{-phenanthroline})]^{2+}$ complex [17]. It is accounted for that the Fe(III)–SiO_2 on irradiation with photon is converted into Fe(II)–SiO_2 that would be complexed with 1,10-phenanthroline in solid state. The binding energy of Fe 2p for the catalyst before and after reaction is shown in Fig. 6. It is observed that the binding energy of Fe $2p_{3/2}$ is slightly shifted to lower BE value from 711.345 to 710.600 eV after irradiation, which is due to the reduction of Fe(III)–SiO_2 to Fe(II)–SiO_2 during the irradiation.

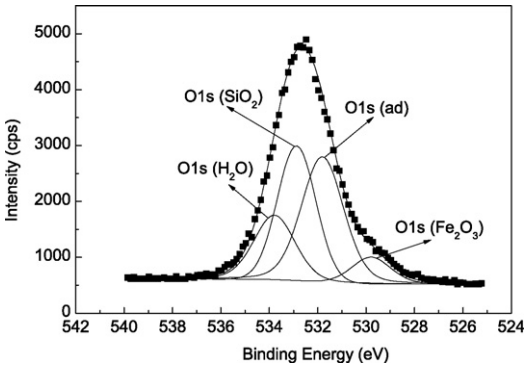

Fig. 4. O 1s curve fitting of S-Fe^{2+}/1 catalyst.

Table 2
XPS data of O element on the surface of the catalysts

Catalysts	Binding energy (eV)				Percentage of O_{ad} or O_L (%)			
	O_{ad}[a]	O_L[b] (SiO_2)	O_L[b] (Fe_2O_3)	O_L[c] (H_2O)	O_{ad}	O_L (SiO_2)	O_L (Fe_2O_3)	O_L (H_2O)
S-Fe^{3+}	531.80	532.80	529.79	533.89	26.94	48.52	2.95	21.59
S-Fe^{3+}/1	531.80	532.80	529.99	533.89	24.16	44.39	3.57	27.87
S-Fe^{3+}/2	531.80	532.84	529.79	533.89	27.73	44.59	7.48	20.2
S-Fe^{2+}	531.80	532.80	529.79	533.89	31.39	42.28	4.36	21.98
S-Fe^{2+}/1	531.81	532.87	529.79	533.79	38.46	34.53	7.60	19.41
S-Fe^{2+}/2	531.89	532.80	529.99	533.70	32.22	30.07	11.93	25.79

[a] The chemisorbed oxygen.
[b] The latter oxygen.
[c] The chemically or physically adsorbed water.

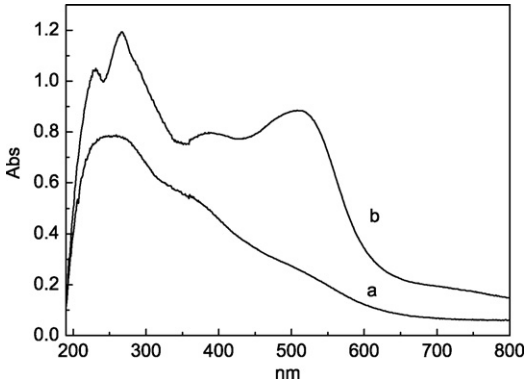

Fig. 5. UV–vis diffuse reflectance spectra of S-Fe^{2+}/1 catalyst: (a) Fe(III)–SiO_2 and (b) Fe(II)–(1,10-phenanthroline)–SiO_2 sample.

3.3. Degradation and mineralization of PAM by heterogeneous photo-Fenton processes

The degradation of 100 mg/L PAM in aqueous solutions under different conditions was preformed by using S-Fe^{2+}/1 as a photo-Fenton catalyst at an initial solution pH of 6.8, and the results are shown in Fig. 7. In the presence of UV lamp, about 5% degradation of PAM in aqueous solution was observed, indicating that the degradation of PAM caused by direct photolysis is very limited. In the presence of 1.0 g/L S-Fe^{2+}/1 catalyst, the removal of PAM was less than 5%, which was caused by the adsorption of PAM on the catalyst. With 1.0 g/L S-Fe^{2+}/1 catalyst and 200 mg/L H_2O_2 in dark, the degradation of PAM was low, implying that the PAM degradation in the course of heterogeneous Fenton reaction is limited in neutral circumstance. In the presence of UV and 200 mg/L H_2O_2 without any catalyst, the concentration of PAM decreased significantly. It is due to the oxidation of PAM by •OH radicals formed direct photolysis of H_2O_2. In the presence of 1.0 g/L S-Fe^{2+}/1 catalyst, UV and 200 mg/L H_2O_2, the concentration of PAM decreased rapidly and about 94% PAM degradation in 90 min. As the leaching of Fe from Fe(III)–SiO_2 catalyst was negligible (described as follows), the degradation of PAM in aqueous solutions was almost caused by the heterogeneous photo-Fenton reaction, indicating that S-Fe^{2+}/1 catalyst exhibits a good photocatalytic activity in PAM degradation. It is assumed that Fe(III) species on the surface of catalysts transform to Fe(II) species under irradiation of UV light, then, the Fe(II) species generate •OH radicals by the decomposition of H_2O_2 [28,29]. At the same time, the UV light irradiates hydrogen peroxide to produce the •OH radicals. Finally, PAM is oxidized by •OH radicals. Therefore, the mechanism for the photo-Fenton degradation of PAM using Fe(III)–SiO_2 catalyst as a heterogeneous catalyst is proposed below:

$$H_2O_2 + h\nu \rightarrow 2^{\bullet}OH \quad (1)$$

$$Fe(III) - X + H_2O + h\nu \rightarrow Fe(II) - X + {}^{\bullet}OH + H^+ \quad (2)$$

$$Fe(II) - X + H_2O_2 \rightarrow Fe(III) - X + OH^- + {}^{\bullet}OH \quad (3)$$

$$PAM + {}^{\bullet}OH \rightarrow \text{Intermediates} \rightarrow CO_2 + H_2O \quad (4)$$

where X represents the surface of Fe(III)–SiO_2 catalyst.

The mineralization process of PAM aqueous solutions under different conditions was measured and the results are shown in Fig. 8. Only with 8 W UV, there was almost no mineralization of PAM. In the present of 1.0 g/L S-Fe^{2+}/1 catalyst and 200 mg/L H_2O_2 in dark, about 20% TOC of PAM was removed after 180 min, indicating that the mineralization of PAM by heterogeneous Fenton reaction is limited in neutral circumstance. In the presence of 8 W UV and 200 mg/L H_2O_2, the mineralization of PAM is significant, about 40%

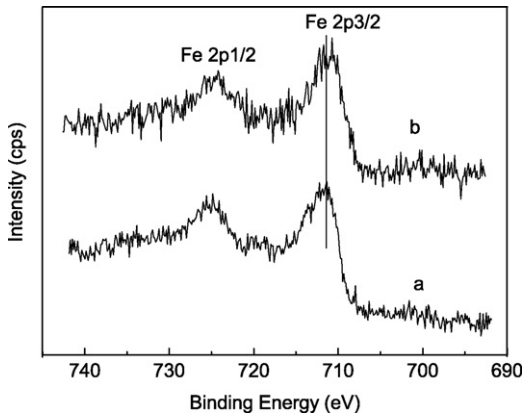

Fig. 6. XPS spectra of the Fe 2p region for the S-Fe^{2+}/1 catalyst: (a) Fe(III)–SiO_2 and (b) Fe(II)–(1,10-phenanthroline)–SiO_2 sample.

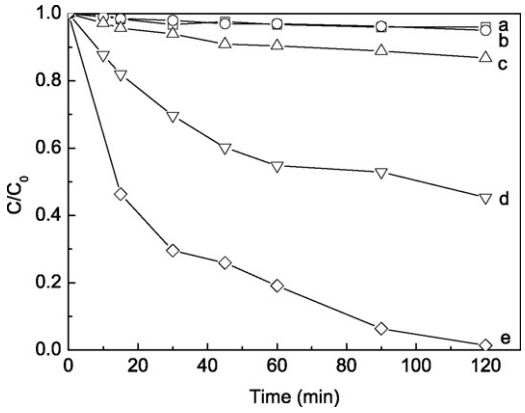

Fig. 7. Degradation of PAM under different conditions: (a) 1 g/L S-Fe^{2+}/1 catalyst, (b) 8 W UV, (c) 1 g/L S-Fe^{2+}/1 catalyst + 200 mg/L H_2O_2, (d) 8 W UV + 200 mg/L H_2O_2 and (e) 8 W UV + 200 mg/L H_2O_2 + 1 g/L S-Fe^{2+}/1 catalyst.

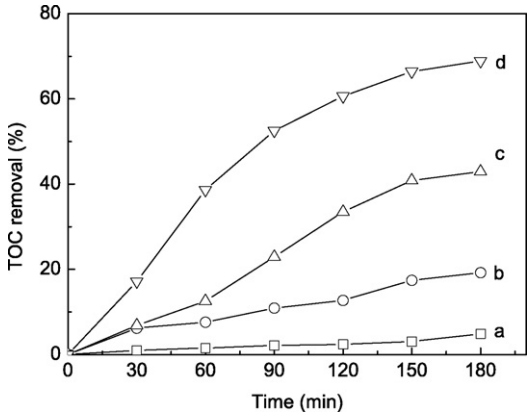

Fig. 8. Mineralization of PAM under different conditions: (a) 8 W UV, (b) 1 g/L S-Fe^{2+}/1 catalyst + 200 mg/L H_2O_2, (c) 8W UV + 200 mg/L H_2O_2 and (d) 8 W UV + 200 mg/L H_2O_2 + 1 g/L S-Fe^{2+}/1 catalyst.

TOC of PAM was removed after 180 min. With the present 1.0 g/L S-Fe^{2+}/1 catalyst, 8 W UV and 200 mg/L H_2O_2, the mineralization of PAM was significantly accelerated. After 180 min, about 70% TOC of PAM was removed, suggesting that the S-Fe^{2+}/1 catalyst show a significant photocatalytic activity for the mineralization of PAM.

3.4. Effects of the precursor species and the OH^-/Fe mole ratio on the PAM degradation

To check the photocatalytic activity of catalysts prepared by different methods, degradation of PAM in aqueous solutions by Fe(III)–SiO_2 catalysts was evaluated and the results are presented in Fig. 9. It was observed that the catalysts prepared with two precursor species and different OH^-/Fe mole ratio showed different photocatalytic activity. At the same OH^-/Fe mole ratio, catalysts prepared with $FeSO_4$ shown a higher photocatalytic activity than $Fe(NO_3)_3$. The most effective catalyst seems to be that prepared with $FeSO_4$ and the OH^-/Fe mole ratio at 1. By using S-Fe^{2+}/1 catalyst, 98.6% of degradation was obtained after 120 min. In contrast, S-Fe^{3+}/1 catalyst gave rise to the less photocatalytic activity, which produced an efficiency degradation of 89.7%. The different photocatalytic activity was observed when two precursors are used. The results are not clear, and it will be the aim of further work (iron oxidation state effect).

3.5. Fe leaching from Fe(III)–SiO_2 catalysts

In addition to having a high photocatalytic activity, stability is another important factor for a catalyst prepared. The concentration of Fe ions in solution with different catalysts was examined by ICP and the results are shown in Fig. 10. It can be seen that there is no significant difference in the patterns of the curves. The concentration of Fe ions increased as reaction time increased, and reached a peak value, then followed by a decrease. The same phenomenon has been reported by Feng et al. [30], but the reason is still not clear. At the same OH^-/Fe mole ratio, the Fe leaching from the catalysts prepared by $Fe(NO_3)_3$ was usually lower than the catalysts prepared by $FeSO_4$. The maximum concentration of Fe among all the catalysts was 0.17 mg/L, suggesting that the Fe leaching from the Fe(III)–SiO_2 catalysts is negligible, and the degradation of PAM aqueous solutions are almost caused by the heterogeneous photo-Fenton reaction in neutral circumstance. After 120 min of the reaction, the percentage of Fe leached from the S-Fe^{2+}/1 catalyst is only about 0.62%, the results also suggest that the catalysts have a long-term stability.

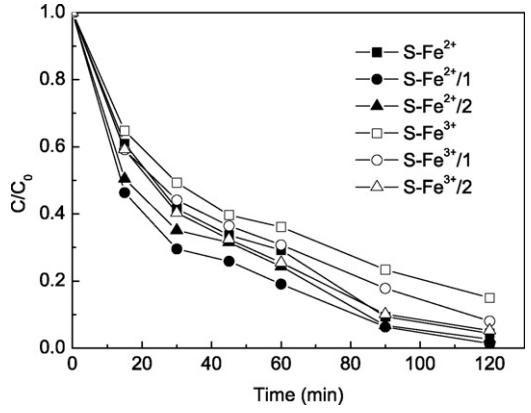

Fig. 9. Degradation of PAM by using different Fe(III)–SiO_2 catalysts.

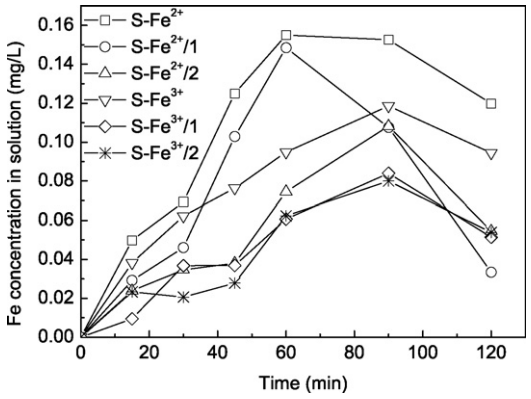

Fig. 10. Fe concentration in solution by using different Fe(III)–SiO_2 catalysts.

4. Conclusions

Fe(III)–SiO_2 catalysts have been synthesized by two methods with $Fe(NO_3)_3$ and $FeSO_4$ as precursors, and were characterized by the BET, XRD and XPS method. The percentage of chemisorbed oxygen on the surface of catalysts prepared by $FeSO_4$ is higher than that prepared by $Fe(NO_3)_3$. The results confirm the formation of Fe(II)–SiO_2 when Fe(III)–SiO_2 was irradiated by photon.

The photocatalytic activities of Fe(III)–SiO_2 catalysts were evaluated by the degradation of PAM from aqueous solution in the photo-Fenton reaction and all the catalysts exhibited a better photocatalytic activities. However, the precursor species and the OH^-/Fe mole ratio have influence on the photocatalytic activities of the catalysts. At the same OH^-/Fe mole ratio, the catalysts could present the better photocatalytic activities when using $FeSO_4$ as precursor. The best efficiency for the degradation of PAM in heterogeneous photo-Fenton reaction was 94% degradation in 90 min and 70% TOC removal in 180 min at an initial pH of 6.8.

Finally, it was observed that Fe leaching from Fe(III)–SiO_2 catalysts was negligible, indicating that the catalysts have a long-term stability and the degradation of PAM from aqueous solution are almost caused by the heterogeneous photo-Fenton reaction.

Acknowledgments

The authors gratefully acknowledge the financial supports from the National Basis Research Foundation of China (973 Program, No. 2004CB418505) and the Research Foundation of Harbin Institute of Technology (No. HIT. MD 2003.02).

References

[1] A. Rho, J. Park, C. Kim, H.K. Yoon, H.S. Suh, Degradation of polyacrylamide in dilute solution, Polym. Degrad. Stab. 51 (1996) 287–293.
[2] M.E. e Silva, E.R. Dutra, V. Mano, J.C. Machado, Preparation and thermal study of polymers derived from acrylamide, Polym. Degrad. Stab. 67 (2000) 491–495.
[3] K. Nakamiya, T. Ooi, S. Kinoshita, Degradation of synthetic water-soluble polymers by hydroquinone peroxidase, J. Ferment. Bioeng. 84 (3) (1997) 218–231.
[4] J.L. Kay-Shoemake, M.E. Watwood, R.D. Lentz, R.E. Sojka, Polyacrylamide as an organic nitrogen source for soil microorganisms with potential effects on inorganic soil nitrogen in agricultural soil, Soil Biol. Biochem. 30 (8/9) (1998) 1045–1052.
[5] S.P. Vijayalakshmi, M. Giridhar, Effect of initial molecular weight and solvents on the ultrasonic degradation of poly(ethylene oxide), Polym. Degrad. Stab. 90 (2005) 116–122.
[6] S.P. Vijayalakshmi, M. Giridhar, Photocatalytic degradation of poly(ethylene oxide) and polyacrylamide, J. Appl. Polym. Sci. 100 (2006) 3997–4003.
[7] G. Ren, D. Sun, J.S. Chunk, Advanced treatment of oil recovery wastewater from polymer flooding by UV/H_2O_2/O_3 and fine filtration, J. Environ. Sci. 18 (2006) 29–32.
[8] C.A. Murray, S.A. Parsons, Removal of NOM from drinking water: Fenton's and photo-Fenton's processes, Chemosphere 54 (2004) 1017–1023.
[9] C. Yardin, S. Chiron, Photo-Fenton treatment of TNT contaminated soil extract solutions obtained by soil flushing with cyclodextrin, Chemosphere 62 (2006) 1395–1402.
[10] S. Parra, L. Henao, E. Mielczarski, Synthesis, testing, and characterization of a novel Nafion membrane with superior performance in photoassisted immobilized Fenton catalysis, Langmuir 20 (2004) 5621–5629.
[11] S. Parra, I. Guasaquillo, O. Enea, E. Melczarski, Abatement of an azo dye on structured C-Nafion/Fe-ion surfaces by photo-Fenton reactions leading to carboxylate intermediates with a remarkable biodegradability increase of the treated solution, J. Phys. Chem. B 107 (2003) 7026–7035.
[12] T. Yuranova, O. Enea, E. Mielczarski, J. Mielczarski, Fenton immobilized photoassisted catalysis through a Fe/C structured fabric, Appl. Catal. B: Environ. 49 (2004) 39–50.
[13] J.H. Ramirez, F.J. Maldonado-Hodar, A.F. Perez-Cadenas, Azo-dye Orange II degradation by heterogeneous Fenton-like reaction using carbon–Fe catalysts, Appl. Catal. B: Environ. 75 (2007) 312–323.
[14] G. Calleja, J.A. Melero, F. Martinez, R. Molina, Activity and resistance of iron-containing amorphous, zeolitic and mesostructured materials for wet peroxide oxidation of phenol, Water Res. 39 (2005) 1741–1750.
[15] F. Martinez, G. Calleja, J.A. Melero, R. Molina, Iron species incorporated over different silica supports for the heterogeneous photo-Fenton oxidation of phenol, Appl. Catal. B: Environ. 70 (2007) 452–460.
[16] F. Martinez, G. Calleja, J.A. Melero, R. Molina, Heterogeneous photo-Fenton degradation of phenolic aqueous solutions over iron-containing SBA-15 catalyst, Appl. Catal. B: Environ. 60 (2005) 181–190.
[17] M. Noorjaha, V.D. Kumari, M. Subrahmanyam, L. Panda, Immobilized Fe(III)–HY: an efficient and stable photo-Fenton catalyst, Appl. Catal. B: Environ. 57 (2005) 291–298.
[18] K. Kusic, N. Koprivanac, I. Selanec, Fe-exchanged zeolite as the effective hetenogeneous Fenton-type catalytic for the organic pollutant minimization: UV irradiation assistance, Chemosphere 65 (2006) 65–73.
[19] J. Feng, X. Hu, P.L. Yue, Effect of initial solution pH on the degradation of Orange II using clay-based Fe nanocomposites as heterogeneous photo-Fenton catalyst, Water Res. 40 (2006) 641–646.
[20] J. Chen, L. Zhu, Heterogeneous UV-Fenton catalytic degradation of dyestuff in water with hydroxyl-Fe pillared bentonite, Catal. Today 126 (2007) 463–470.
[21] J. Feng, X. Hu, P.L. Yue, Degradation of azo-dye Orange II by a photoassisted Fenton reaction using a novel composite of iron oxide and silicate nanoparticles as a catalyst, Ind. Eng. Chem. Res. 42 (2003) 2058–2066.
[22] J.H. Ramirez, C.A. Costa, L.M. Madeira, Fenton-like oxidation of Orange II solutions using heterogeneous catalysts based on saponite clay, Appl. Catal. B: Environ. 71 (2007) 44–56.
[23] M.W. Scoggins, J.W. Miller, Spectrophotometric determination of water soluble organic amides, Anal. Chem. 47 (1975) 152–154.
[24] M. Charles, J.R. Flynn, Hydrolysis of inorganic iron(III) salts, Chem. Rev. 84 (1984) 31–41.
[25] B.J. Tan, K.J. Klabunde, P.M.A. Sherwood, X-ray photoelectron spectroscopy studied of solvated metal atom dispersed catalysts-monometallic iron and bimetallic iron cobalt particles on alumina, Chem. Mater. 2 (1990) 186–191.
[26] H. Chen, A. Sayari, A. Adnot, F. Larachi, Composition-activity effects of Mn–Ce–O composites on phenol catalytic wet oxidation, Appl. Catal. B: Environ. 32 (2001) 195–204.
[27] Y. Liu, D. Sun, Effect of CeO_2 doping on catalytic activity of Fe_2O_3/γ-Al_2O_3 catalyst for catalytic wet peroxide oxidation of azo dyes, J. Hazard. Mater. 143 (2007) 448–454.
[28] C. Hsueh, Y. Huang, C. Wang, Photoassisted Fenton degradation of non-biodegradable azo-dye (Reactive Black 5) over a novel supported iron oxide catalyst at neutral pH, J. Mol. Catal. A: Chem. 245 (2006) 78–86.
[29] P. Mazellier, B. Sulzberger, Diuron degradation in irradiated, heterogeneous iron/oxalate systems: the rate-determining step, Environ. Sci. Technol. 35 (2001) 3314–3320.
[30] J. Feng, X. Hu, P.L. Yue, Discoloration and mineralization of orange using different heterogeneous catalysts containing Fe: a comparative study, Environ. Sci. Technol. 38 (2004) 5773–5778.